Available online at www.sciencedirect.com
ScienceDirect
Journal of Molecular Graphics and Modelling 25 (2007) 806–812
Journal of Molecular Graphics and Modelling
www.elsevier.com/locate/JMGM

Computation of through-space NMR shielding effects by aromatic ring–cation complexes: Substantial synergistic effect of complexation

Ned H. Martin *, Kristin L. Main, Amy K. Pyles

Department of Chemistry and Biochemistry, University of North Carolina Wilmington, 601 S. College Road, Wilmington, NC 28403-5932, United States

Received 20 June 2006; accepted 1 August 2006
Available online 7 September 2006

Abstract

The HF-GIAO method in Gaussian 03 was employed to calculate the NMR isotropic shielding values of a diatomic hydrogen probe and to predict the through-space proton NMR shielding increment surfaces above benzene complexed with ammonium, lithium, sodium, potassium, magnesium or calcium ion. The sum of the calculated isotropic shielding values for the proximal hydrogen of a diatomic hydrogen probe over benzene and those calculated at appropriate positions relative to cations were subtracted from the isotropic shielding values calculated for the complexes. The result is a shielding increment for complexation. Complexation results in a synergistic effect on NMR shielding. Enhanced shielding was observed over the π electron cloud of benzene upon complexation with the cations, more than the sum of the separate effects of the aromatic ring and the charge. The results are interpreted in terms of polarization of the π cloud of benzene by the cation and its consequences.

Keywords: NMR; Through-space shielding effects; GIAO; Benzene; Benzene–cation complex; Synergistic shielding effect

1. Introduction

Complexes between cations and aromatic rings of amino acids in peptides are important in many biological systems [1]. Ma and Daugherty [2] have written an excellent review of the physical chemical aspects and has cited numerous biological examples of noncovalent cation–π interactions. Among the many significant biological examples is the voltage-gated potassium ion channel which relies on a cation–π interaction between potassium ion and the aromatic ring of tyrosine [3,4]. In a study of the amino acid sequences in the pore region of the potassium ion channel from various sources it was found that a highly conserved Gly-Tyr-Gly (GYG) sequence appears to be essential for ion selectivity [5]. Sodium channels are also thought to involve cation–π complexes between phenylalanine or tyrosine and sodium ion; neurotoxins such as tetrodotoxin and saxitoxin interfere with this process by providing a guanidinium ion that competitively binds to the aromatic residues and prevents the proper functioning of the ion channel [6].

Cation–π complexes have been found in human acetylcholinesterase [7] and butyrylcholinesterase [8]. A possible cation–π interaction involving Mg^{2+} in HIV integrase has been reported [9]. HIV integrase is an enzyme essential for replication of the virus [10]. Another example of a protein having aryl–cation complexes is the recently discovered bacterial protein that transports ammonia across cell membranes as ammonium ion complexed to a tyrosine residue [11].

We have previously reported the results of HF-GIAO calculations to calculate through-space NMR shielding effects, to map the resulting through-space NMR shielding increments, and to develop through-space NMR shielding equations for a number of common organic functional groups, including the benzene ring [12,13], the carbon–carbon double bond [14–17], the carbon–carbon triple bond, the carbon–nitrogen triple bond, the nitro group [18], the carbonyl group [19], and functional groups common to peptides [20]. Recently, we reported the NMR shielding surfaces of some simple aromatic and antiaromatic hydrocarbons [21]. The shielding predictions

* Corresponding author. Tel.: +1 910 962 3453; fax: +1 910 962 3013.
E-mail address: martinn@uncw.edu (N.H. Martin).

1093-3263/$ – see front matter
doi:10.1016/j.jmgm.2006.08.001

derived from calculations of small molecule models of those functional groups proved to be successful at accurately predicting through-space chemical shift effects in more complex molecules that contained those functional groups. We now report our computational study of the through-space NMR shielding of a diatomic hydrogen probe molecule by cation–aromatic ring π complexes. Knowledge of these through-space shielding effects should aid in the structure determination of peptides and other molecules that possess these structural features.

2. Computational methods

Models of π–complexes of benzene and the cations listed in Fig. 1 were built in Titan [22] on a Dell Dimension 3.31 GHz pc and a geometry optimization calculation was performed at the Hartree–Fock level of theory using a 6–31G(d, p) basis set [23]. In each case, the optimum geometry of the complex had the cation over the center of the benzene ring. Equilibrium distances between the plane of benzene and each cation are shown in Table 1. A diatomic hydrogen (H_2) probe [24], previously geometry optimized at HF/6–31G(d, p), was placed along the *Z* axis (perpendicular to the ring) with the proximal hydrogen at a distance of 2.5 Å from the plane of the carbon atoms of benzene on the side of the ring opposite the cation (Fig. 2). A series of single point NMR calculations was performed in Gaussian 03 [25] on these supramolecules using the same method and basis set, moving the H_2 in 1.0 Å increments in both the *X* and *Y* directions in separate calculations. The process was repeated with the H_2 probe at proximal hydrogen distances of 3.0 and 4.0 Å from the plane of the carbon atoms of benzene. These calculations covered a 3 Å × 3 Å grid in one quadrant. Symmetry allowed only one quadrant (two in the case of NH_4^+) to be calculated and the data to be replicated by a reflection across the *X* and *Y* (or only the *X* for NH_4^+) axis. Each of these structures was oriented with the benzene ring in the *XY* plane with the center of the ring at the origin of Cartesian space.

NH_4^+ Li^+ Na^+ K^+ Mg^{2+} Ca^{2+}

Fig. 1. Cations used in this study.

Table 1
Isotropic shielding increment values (ppm) of the H_2 probe at 2.5, 3.0, and 4.0 Å above the center of the plane of benzene (alone) or benzene complexed with selected cations

Cation	Equilibrium distance from benzene (Å)	Maximum shielding increment (ppm)		
		2.5 Å	3.0 Å	4.0 Å
None	n/a	2.97	1.83	0.84
NH_4^+	3.168[a]	3.38	2.17	1.09
Li^+	1.949	3.64	2.42	1.26
Na^+	2.452	3.66	2.40	1.24
K^+	3.035	3.61	2.34	1.18
Mg^{2+}	1.988	4.49	3.32	1.78
Ca^{2+}	2.583	4.20	2.86	1.57

[a] Distance to N; proximal H is 2.151 Å from ring.

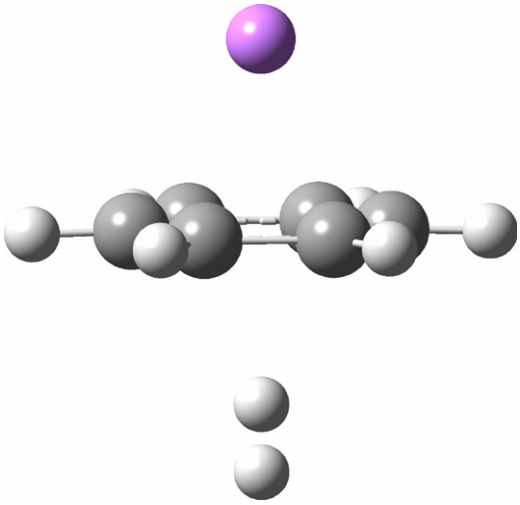

Fig. 2. General structure of the metal cation–benzene complex with a diatomic hydrogen probe molecule.

The shielding increment ($\Delta\sigma$) at a given point in Cartesian space was determined by subtracting the calculated isotropic shielding value of one of the hydrogens in the H_2 probe alone from the isotropic shielding value of the proximal hydrogen of the H_2 probe in the cation–benzene π complex. Isotropic shielding values of the complexed H_2 that are greater than the calculated isolated H_2 isotropic shielding value (26.77 ppm) produce positive (shielding) $\Delta\sigma$ values, and those with smaller values lead to negative (deshielding) $\Delta\sigma$ values. The shielding increments ($\Delta\sigma$) are therefore equal in magnitude but opposite in sign to differences in ^{1}H NMR chemical shifts ($\Delta\delta$). Three-dimensional NMR shielding increment surfaces ($\Delta\sigma$ versus *X* and *Y* at a fixed value of *Z*) were prepared using TableCurve 3D [26] to represent graphically the locations and magnitudes of shielding and deshielding regions over the cation–benzene π complexes in the study. Similar calculations were performed on a cation and a diatomic hydrogen probe, but without benzene. Previously reported results of shielding calculations of H_2 over benzene [21] were also used. The counterpoise method [27] was employed to estimate the basis set superposition error (BSSE); in no case did the value of the shielding change by more than 0.05 ppm; this is well below the uncertainty in the method (0.10 ppm), and was ignored.

3. Results and discussion

Shielding increment surfaces for a diatomic hydrogen probe on the side of benzene opposite a complexed Mg^{2+} are shown in Fig. 3. The surfaces range from pointed mounds of shielding for a probe near the ring to flattened mounds as the distance between the ring and the probe increases. The maximum shielding increment for the complex, in all cases observed over the center of the ring, diminishes with distance of the probe from the plane of the ring (maximum $\Delta\sigma$ is 4.49 ppm at 2.5 Å, diminishing to 1.78 ppm at 4.0 Å).

The shapes of the shielding increment surfaces are similar for complexes with the other metal cations, with the major difference being the magnitude of maximum shielding. In

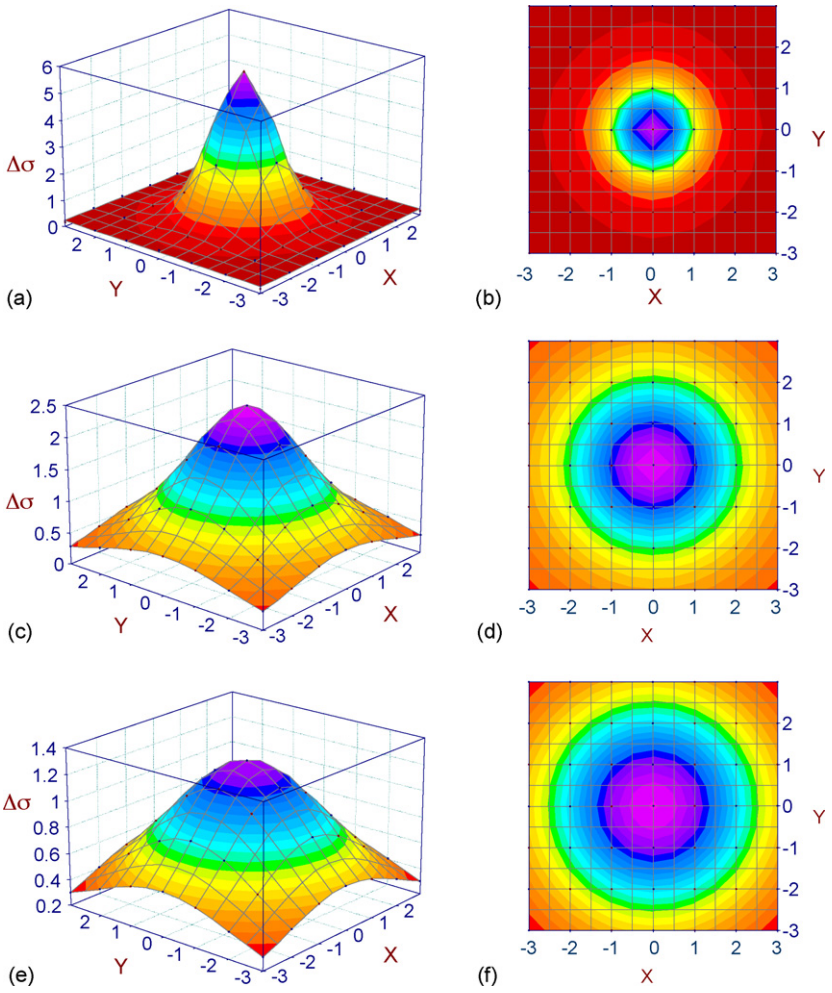

Fig. 3. Calculated isotropic NMR shielding increment surfaces (ppm) of a magnesium ion–benzene complex using a diatomic hydrogen as the probe molecule at (a) 2.5 Å side view, (b) 2.5 Å top view, (c) 3.0 Å side view, (d) 3.0 Å top view, (e) 4.0 Å side view, (f) 4.0 Å top view.

general, doubly charged ions (Mg^{2+} and Ca^{2+}) showed greater shielding effects than singly charged ions (Li^+, Na^+, K^+ and ammonium), as expected. The maximum shielding increment ($\Delta\sigma$) at several distances of the H_2 probe above benzene complexed with various cations is shown in Table 1.

Complexes of benzene and ammonium ion, with its more dispersed charge, give much flatter shielding surfaces (Fig. 4) and smaller maximum shielding values than metal ion complexes.

Complexation of a cation to an aromatic ring results in enhanced shielding of a covalently bonded probe molecule (H_2) on the side of the ring opposite the cation. The observed shielding of the H_2 probe includes the shielding effects of both the cation (due to its charge) and the aromatic ring, due primarily to its ring current effect. To investigate the nature of the shielding effect in more detail, the shielding increments of H_2 over benzene (alone) and of H_2 at fixed distances from each cation (oriented as in the complexes) were subtracted from the shielding increments of H_2 on the side opposite the cation in the benzene–cation complex. The result is a shielding increment surface entirely due to complexation. Fig. 5 shows this graph for Mg^{2+}.

The other metal cations gave similarly shaped surfaces, although with less shielding. Two observations are noteworthy. First, the magnitude of the shielding effect *entirely due to complexation* is substantial, greater than 0.5 ppm for H_2 at 2.5 Å above the plane of the carbons of benzene complexed to Mg^{2+}. That is, complexation of a metal ion to an aromatic ring enhances the shielding effect on a covalently bonded hydrogen on the side of the ring opposite the metal ion substantially compared to the sum of the isolated effects of the aromatic ring and the metal ion. Second, the shape of the complexation shielding surface at a distance of 2.5 Å from the plane of the benzene ring carbons is a mound of shielding with a deep depression in the center. This shape can be understood in terms of a simple π polarization model and the consequent effects on shielding. Complexation of benzene with a cation polarizes the π electrons of benzene. An example of this can be seen in Fig. 6, where the graphic of the HOMO of benzene, the HOMO of a benzene–Mg^{2+} complex, and the two superimposed clearly shows how complexation increases the coefficient of the lobe of the HOMO closest to the metal cation while diminishing that opposite the cation. Relative to benzene, the decreased π electron density on the side of the complexed benzene ring opposite the cation polarizes the covalent bond of diatomic hydrogen, increasing the electron density near the proximal hydrogen, with the consequence that

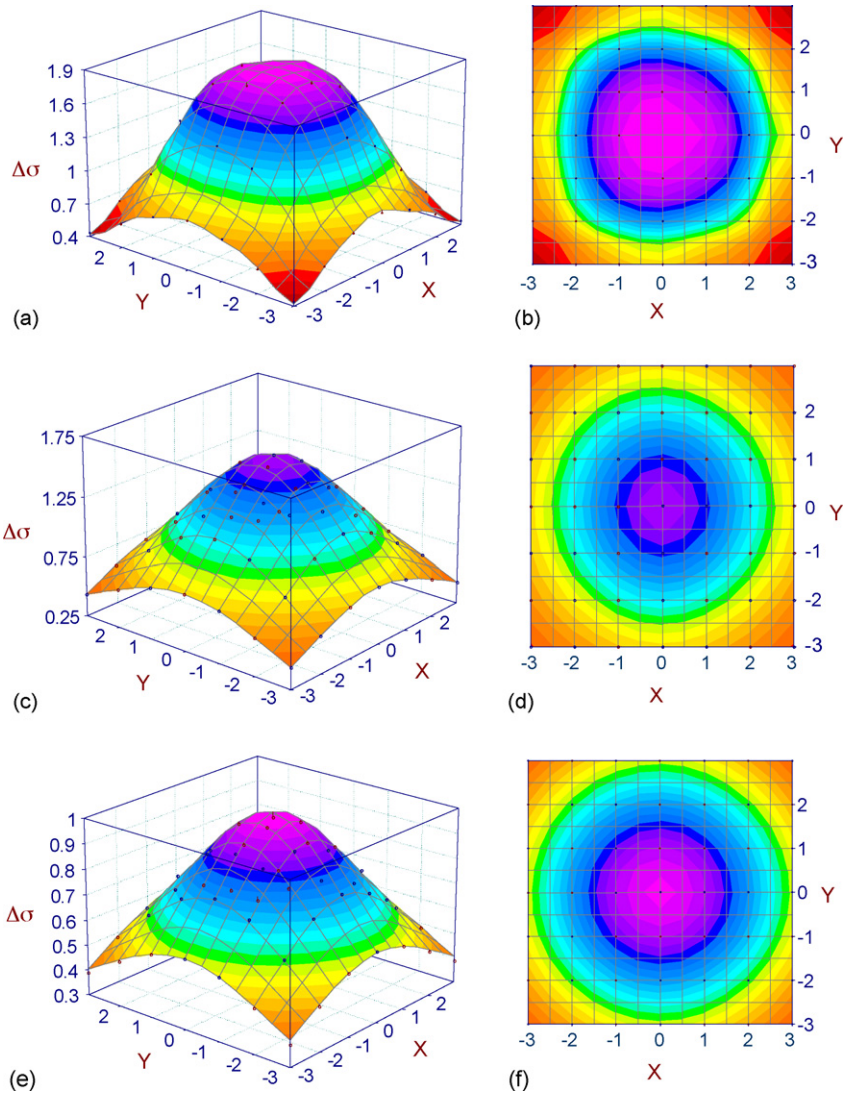

Fig. 4. Calculated isotropic NMR shielding increment surfaces (ppm) of an ammonium ion–benzene complex using a diatomic hydrogen as the probe molecule at (a) 2.5 Å side view, (b) 2.5 Å top view, (c) 3.0 Å side view, (d) 3.0 Å top view, (e) 4.0 Å side view, (f) 4.0 Å top view.

the proximal hydrogen becomes more shielded. However, superimposed on that general increase in shielding is another factor. The high electron density of the π cloud of benzene causes slight electrostatic deshielding of a probe in the proximity of the π cloud. This effect is usually obscured by the much larger shielding effect of the aromatic ring current. The ring current effect is greatest over the center of the ring, and falls off with increasing radial distance from the central axis of the ring.

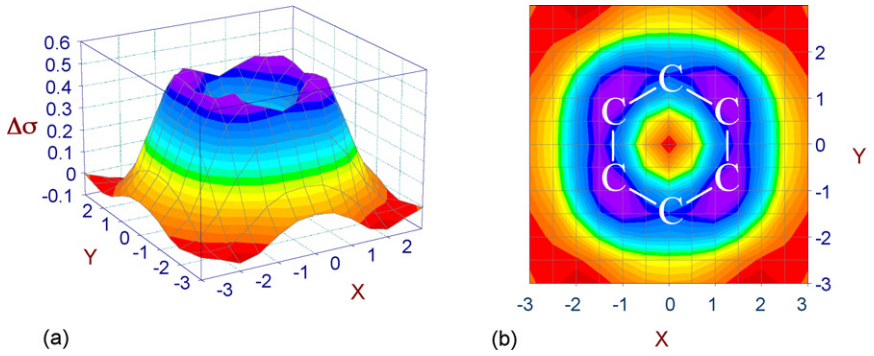

Fig. 5. Calculated net isotropic NMR shielding surface (ppm) due to complexation, calculated by subtracting the isotropic shielding increments of benzene and those of Mg^{2+} from those of benzene complexed with Mg^{2+} using diatomic hydrogen as the probe molecule at (a) 2.5 Å side view and (b) 2.5 Å top view with benzene carbon positions shown.

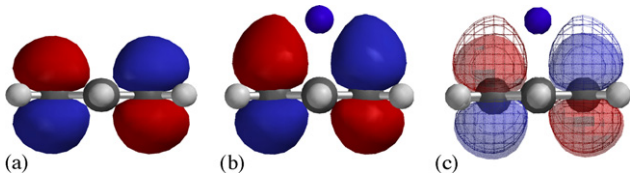

Fig. 6. Graphical representations of (a) the HOMO of benzene, (b) the HOMO of a benzene–Mg^{2+} complex, and (c) the two HOMOs superimposed, with atoms are represented by spheres.

Complexation of benzene with a cation causes polarization of the π cloud, and the diminished electron density on the side of the ring near the hydrogen probe (opposite the cation) results in a reduced electrostatic deshielding effect on the probe molecule near the π cloud. This diminished deshielding (i.e., enhanced shielding) effect is localized in the vicinity of the π electron cloud. The general shielding effect of the ring current is also diminished on the side of the ring opposite the cation, with the greatest decrease in shielding localized over the center of the ring. The consequence is a mound of shielding with a depression in the center. The outline of the maximum shielding region closely matches the circular shape and radial extent of the π cloud of electrons, clearly seen in Fig. 5. The apparent four-fold symmetry is a graphical artifact of spacing the data points 1.0 Å apart and of replicating the data over four quadrants, and should be ignored.

Table 2 lists the isotropic shielding increment on a diatomic hydrogen probe 2.5 Å above one of the benzene ring carbons (the approximate position of maximum shielding due to complexation, as seen in Fig. 5) in each of the cation–benzene complexes, the shielding due to the same position and orientation relative to the cation alone, the sum of the cation shielding increment plus the shielding increment of uncomplexed benzene, and the difference between that sum and the complex. This difference, which we term the synergistic shielding effect, can be substantial (up to 0.6 ppm), especially for the ions of 2+ charge. The ammonium ion complex has the smallest synergistic shielding effect, as expected because of its dispersed charge.

Table 4
Natural (npa) charges of the proximal hydrogen of probe molecule at 2.5 Å above the center of the plane of benzene (alone) or benzene complexed with selected cations, and npa charges above one of the carbons of benzene or a benzene–cation complex

Cation	npa Charge over ring center	npa Charge over one carbon
None	+0.014	+0.010
NH_4^+	−0.020	−0.021
Li^+	−0.040	−0.039
Na^+	−0.045	−0.031
K^+	−0.023	−0.023
Mg^{2+}	−0.091	−0.087
Ca^{2+}	−0.072	−0.069

Complexation of benzene with a cation distorts the geometry of the benzene ring. The hydrogen atoms are bent out of the plane of the ring carbons and away from the cation. There are also minor distortions of bond lengths. In an effort to determine what effect the ring distortion has on shielding, calculations were performed using the distorted rings and a diatomic hydrogen probe placed 2.5 Å over one of the ring carbons, but without a cation. The isotropic shielding value of a diatonic hydrogen probe over (undistorted) benzene was subtracted from the shielding values obtained from the distorted rings, resulting in a $\Delta\sigma$ due to ring distortion. These values are collected in Table 3. The calculated percent of this value relative to the synergistic $\Delta\sigma$

Table 2
Isotropic shielding increment values (ppm) for a diatomic hydrogen probe over one of the benzene ring carbon atoms at a distance 2.5 Å above the plane of the ring carbons in cation–benzene complexes, in the same position relative to the cations but in the absence of benzene, the sum of the cation shielding increment plus the shielding increment of (uncomplexed) benzene, and the difference between that sum and the complex

Cation	Shielding increment, complex	Shielding increment, cation only	Sum of shielding increments, cation only and benzene only	Synergistic $\Delta\sigma$: difference, complex–sum
NH_4^+	1.51	0.39	1.44	0.07
Li^+	1.87	0.61	1.66	0.21
Na^+	1.84	0.52	1.58	0.26
K^+	1.70	0.46	1.52	0.18
Mg^{2+}	2.79	1.16	2.22	0.57
Ca^{2+}	2.38	0.97	2.03	0.35

Table 3
Deviation of the ring hydrogens from the plane of the carbons in the ring (Å), the shielding increment ($\Delta\sigma$, ppm) over one carbon of the ring due to ring distortion, and the percentage of the synergistic shielding increment over one carbon due to ring distortion (%)

Cation	Deviation of hydrogens from plane of carbons	$\Delta\sigma$ due to ring distortion	Percentage of synergistic $\Delta\sigma$ from ring distortion
NH_4^+	0.025	0.009	13
Li^+	0.012	0.004	2
Na^+	0.031	0.020	8
K^+	0.035	0.021	12
Mg^{2+}	0.026	0.005	9
Ca^{2+}	0.061	0.035	10

Table 5
Natural population analysis charges of the proximal hydrogen of the H_2 probe at a position 2.5 Å over one carbon of the benzene ring in the complexes but without the benzene ring, the npa charge over one carbon in the complex (Table 3 minus the npa charge at that position relative to the cation in the complex (but without the benzene) minus the npa charge over one carbon of benzene, and their ratio expressed as a percentage (%)

Cation	Cation-only npa charge at the position over one carbon of the ring, but without benzene	Difference in npa charge at that position (complex minus cation minus benzene)	Percentage of charge due to complexation
NH_4^+	−0.026	0.004	25
Li^+	−0.039	0.010	27
Na^+	−0.032	0.009	29
K^+	−0.026	0.006	28
Mg^{2+}	−0.077	0.020	23
Ca^{2+}	−0.062	0.017	25

listed in Table 2 is also shown in Table 3. These percentages range from 2 to 13%, with the larger percentages associated with the larger cations, as expected. Therefore, although benzene ring distortion due to complexation may contribute to the synergistic shielding effect, it is not a major factor.

Weinhold natural population analysis (npa) charges [28–30] on the proximal hydrogen of the probe molecule at a distance of 2.5 Å over the center of the plane of the carbon atoms of benzene and benzene–cation complexes, and 2.5 Å over one of the ring carbon atoms are listed in Table 4. A graph of the maximum shielding increment versus npa charge on the proximal hydrogen of the probe molecule at 2.5 Å at the two positions relative to benzene and the cation–benzene complexes is shown in Fig. 7 (squares = over ring center; triangles = over one carbon). Each plot is linear, with $r^2 = 0.98$, showing the expected high linear correlation between shielding and electron density.

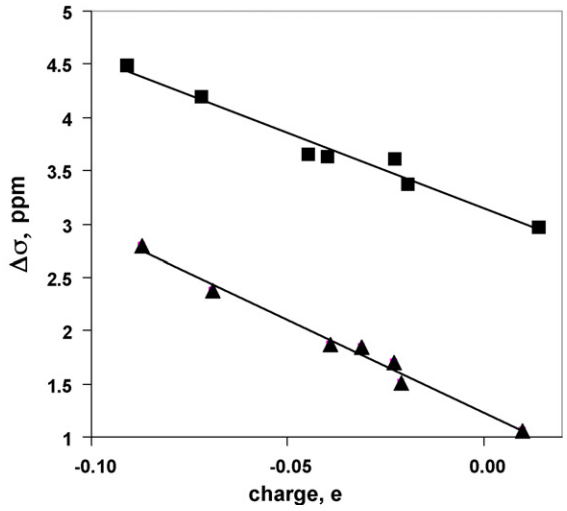

Fig. 7. Graph of the shielding increment ($\Delta\sigma$) 2.5 Å over one carbon of the benzene ring in cation–benzene complexes (ppm) vs. the calculated natural population analysis charge on the proximal hydrogen of the H_2 probe.

Table 6
Polarization-induced shielding increment ($\Delta\sigma$, ppm) of the proximal hydrogen of the H_2 probe molecule at 2.5 Å above one carbon of benzene complexed with selected cations, and the synergistic shielding increment (ppm) of the benzene–cation complexes

Cation	Polarization-induced $\Delta\sigma$	Synergistic $\Delta\sigma$
NH_4^+	0.11	0.07
Li^+	0.22	0.21
Na^+	0.23	0.26
K^+	0.18	0.18
Mg^{2+}	0.40	0.57
Ca^{2+}	0.33	0.35

Table 5 lists the npa charges calculated for the proximal hydrogen of the H_2 probe at a position over each cation at a location comparable to 2.5 Å over one carbon of benzene ring of a complex (but with just the cation present, not the aromatic ring), and the difference between it and the sum of the charge over a ring carbon of the corresponding complex plus the charge over one carbon of benzene alone. The ratio of this value to the npa charge of the complex, expressed as a percentage, is remarkably constant at 26 ± 3% for each of the cations. Thus, complexation introduces polarization of the H_2 probe in addition to that caused by the cation and the benzene ring. Fig. 7 shows that shielding is linearly related to charge for the proximal hydrogen of the probe molecule. Therefore, the amount of shielding increment derived from the complexation-induced polarization (i.e., polarization arising from other than the cation and the benzene ring contributions) can be estimated by multiplying the difference in shielding increment 2.5 Å over one benzene ring carbon in the complex relative to benzene alone (using values from Table 2) by the percentage of charge due to complexation. In Table 6, this product is compared with the synergistic $\Delta\sigma$ from Table 2. The two numbers are very similar, differing by less than the uncertainty in our method (0.10 ppm). This suggests that complex-induced polarization is the major contributor to the synergistic shielding effect.

4. Conclusions

Diatomic hydrogen was used as a computational probe to examine the effect of complexation of cations with benzene on the calculated NMR isotropic shielding value over the benzene ring on the side of the ring opposite the cation. Both benzene and cations cause shielding of a hydrogen probe. The calculated shielding increment of a hydrogen probe over selected positions of a benzene ring complexed to a cation is substantially greater than the sum of the calculated shielding increments due to benzene or a cation alone. Complexation therefore has a

synergistic effect on NMR shielding. Most of the effect is due to polarization of the probe by the complex in addition to the polarization caused by the cation. Some of the effect can be attributed to distortion of the benzene ring upon complexation. The shape of the shielding increment surface of benzene–cation complexes can be understood in terms of polarization of the π cloud of benzene and its consequences.

References

[1] R.F. Castellano, F. Diederich, E.A. Meyer, Interactions with aromatic rings in chemical and biological recognition, Angew. Chem. Int. Ed. 42 (11) (2003) 1210–1250.

[2] J.C. Ma, D.A. Dougherty, The cation–π interaction, Chem. Rev. 97 (1997) 1303–1324.

[3] C. Miller, Ion channel structure and function, Science 258 (1992) 240–241.

[4] D. Dougherty, Cation–p interactions in chemistry and biology: a new view of benzene, Phe, Tyr, and Trp, Science 271 (1996) 163–168.

[5] L. Heginbotham, R. MacKinnon, The aromatic binding site for tetraethylammonium ion on potassium channels, Neuron 8 (1992) 483–491.

[6] J. Satin, J.W. Kyle, M. Chen, P. Bell, L.L. Cribbs, H.A. Fozzard, R.B. Rogart, A mutant of TTX-resistant cardiac sodium channels with TTX-sensitive properties, Science 256 (1992) 1202–1205.

[7] J.L. Sussman, M. Harel, F. Frolow, C. Oefner, A. Goldman, L. Toker, I. Silman, Atomic structure of acetylcholinesterase from Torpedo, Californica: a prototypic acetylcholine-binding protein, Science 253 (1991) 872–879.

[8] P. Masson, P. Legrand, C.F. Bartels, M.T. Froment, L.M. Schopher, O. Lockridge, Role of aspartate 70 and tryptophan 82 in binding of succinyldithiocholine to human butyrylcholinesterase, Biochemistry 36 (1997) 2266–2277.

[9] M.C. Nicklaus, N. Neamati, H. Hong, A. Mazumder, S. Sunder, J. Chen, G.W.A. Milne, Y. Pommier, HIV-1 integrase pharmacophore: discovery of inhibitors through three-dimensional database searching, J. Med. Chem. 40 (1997) 920–929.

[10] M. Taktakishvili, N. Neamati, Y. Pommier, S. Pal, V. Nair, Recognition and inhibition of HIV integrase by novel dinucleotides, J. Am. Chem. Soc. 122 (24) (2000) 5671–5677.

[11] M.A. Knepper, P. Agre, Structural biology: the atomic architecture of a gas channel, Science 305 (2004) 1573–1574.

[12] N.H. Martin, N.W. Allen III, K.D. Moore, L. Vo, A proton NMR shielding model for the face of a benzene ring, J. Mol. Struct. (Theochem.) 454 (1998) 161–166.

[13] N.H. Martin, N.W. Allen III, J.C. Moore, An algorithm for predicting NMR shielding of protons over substituted benzene rings, J. Mol. Graphics Mod. 18 (3) (2000) 242–246.

[14] N.H. Martin, N.W. Allen III, E.K. Minga, S.T. Ingrassia, J.D. Brown, An empirical proton NMR shielding equation for alkenes based on ab initio calculations, Struct. Chem. 9 (6) (1998) 403–410.

[15] N.H. Martin, N.W. Allen, III, E.K. Minga, S.T. Ingrassia, J.D. Brown, Proceedings of ACS Symposium "Modeling NMR Chemical Shifts: Gaining Insights into Structure and Environment," ACS Press, 1999.

[16] N.H. Martin, N.W. Allen III, E.K. Minga, S.T. Ingrassia, J.D. Brown, An improved model for predicting proton NMR shielding by alkenes based on ab initio GIAO calculations, Struct. Chem. 10 (5) (1999) 375–380.

[17] N.H. Martin, N.W. Allen III, S.T. Ingrassia, J.D. Brown, E.K. Minga, An algorithm for predicting proton deshielding over a carbon–carbon double bond, J. Mol. Graphics Model. 18 (1) (2000) 1–6.

[18] N.H. Martin, K.H. Nance, Modeling through-space magnetic shielding over the ethynyl, cyano, and nitro groups, J. Mol. Graphics Model. 21 (2002) 51–56.

[19] N.H. Martin, N.W. Allen III, J.D. Brown, D.M. Kmiec Jr., L. Vo, An NMR shielding model for protons above the plane of a carbonyl group, J. Mol. Graphics Model. 22 (2003) 127–131.

[20] N.H. Martin, D.M. Loveless, K.L. Main, A.K. Pyles, Computation of through-space shielding effects by functional groups common to peptides, J. Mol. Graphics Model., in press.

[21] N.H. Martin, D.M. Loveless, K.L. Main, D.C. Wade, Computation of through-space NMR shielding effects by small-ring aromatic and anti-aromatic hydrocarbons, J. Mol. Graphics Model., in press.

[22] Titan, Version 1.0.1, Wavefunction, Inc., Schrödinger, Inc., 1999.

[23] W.J. Hehre, L. Radom, P.V.R. Schleyer, J.A. Pople, Ab Initio Molecular Orbital Theory, Wiley, New York, 1986.

[24] N.H. Martin, D.M. Loveless, D.C. Wade, A comparison of the calculated NMR shielding probes, J. Mol. Graphics Model. 23 (2004) 285–290.

[25] Gaussian 03, Revision B.01, M.J. Frisch, G.W. Trucks, H.B. Schlegel, G.E. Scuseria, M.A. Robb, J.R. Cheeseman, J.A. Montgomery, Jr., T. Vreven, K.N. Kudin, J.C. Burant, J.M. Millam, S.S. Iyengar, J. Tomasi, V. Barone, B. Mennucci, M. Cossi, G. Scalmani, N. Rega, G.A. Petersson, H. Nakatsuji, M. Hada, M. Ehara, K. Toyota, R. Fukuda, J. Hasegawa, M. Ishida, T. Nakajima, Y. Honda, O. Kitao, H. Nakai, M. Klene, X. Li, J.E. Knox, H.P. Hratchian, J.B. Cross, C. Adamo, J. Jaramillo, R. Gomperts, R.E. Stratmann, O. Yazyev, A.J. Austin, R. Cammi, C. Pomelli, J.W. Ochterski, P.Y. Ayala, K. Morokuma, G.A. Voth, P. Salvador, J.J. Dannenberg, V.G. Zakrzewski, S. Dapprich, A.D. Daniels, M.C. Strain, O. Farkas, D.K. Malick, A.D. Rabuck, K. Raghavachari, J.B. Foresman, J.V. Ortiz, Q. Cui, A.G. Baboul, S. Clifford, J. Cioslowski, B.B. Stefanov, G. Liu, A. Liashenko, P. Piskorz, I. Komaromi, R.L. Martin, D.J. Fox, T. Keith, M.A. Al-Laham, C.Y. Peng, A. Nanayakkara, M. Challacombe, P.M.W. Gill, B. Johnson, W. Chen, M.W. Wong, C. Gonzalez, J.A. Pople, Gaussian, Inc., Pittsburgh, PA, 2003.

[26] TableCurve3D, Version 3.00A, AISN Software, San Rafael, CA, 1997.

[27] S.F. Boys, F. Bernardi, The calculations of small molecular interaction by the difference of separate total energies. Some procedures with reduced error, Mol. Phys. 19 (1970) 553–566.

[28] A.E. Reed, R.B. Weinstock, F. Weinhold, J. Chem. Phys. 83 (1985) 735–746.

[29] A.E. Reed, L.A. Curtiss, F. Weinhold, Chem. Rev. 88 (1988) 899–926.

[30] J.E. Carpenter, F. Weinhold, J. Mol. Struct. (Theochem.) 169 (1988) 41–62.